

EllipBench: A Large-scale Benchmark for Machine-learning based Ellipsometry Modeling

Yiming Ma^{*1} Xinjie Li^{*2} Xin Sun³ Zhiyong Wang³ Lionel Z. WANG¹

Abstract

Ellipsometry is used to indirectly measure the optical properties and thickness of thin films. However, solving the inverse problem of ellipsometry is time-consuming since it involves human expertise to apply the data fitting techniques. Many studies use traditional machine learning-based methods to model the complex mathematical fitting process. In our work, we approach this problem from a deep learning perspective. First, we introduce a large-scale benchmark dataset to facilitate deep learning methods. The proposed dataset encompasses 98 types of thin film materials and 4 types of substrate materials, including metals, alloys, compounds, and polymers, among others. Additionally, we propose a deep learning framework that leverages residual connections and self-attention mechanisms to learn the massive data points. We also introduce a reconstruction loss to address the common challenge of multiple solutions in thin film thickness prediction. Compared to traditional machine learning methods, our framework achieves state-of-the-art (SOTA) performance on our proposed dataset. The dataset and code will be available upon acceptance.

1. Introduction

Thin films play a pivotal role in modern technology and are used in a wide range of industries, including optoelectronic devices, microelectronics, energy, and aerospace. The optical properties of thin films, especially the refractive index and extinction coefficient, are crucial for the design of high-performance devices. Ellipsometry is a traditional method to measure the optical properties and thickness of thin films (Fujiwara, 2007). The principle of ellipsometry for measuring the optical properties and thickness of thin films is shown in Figure 1. The advantages of ellipsometry are the

^{*}Equal contribution ¹The Hong Kong Polytechnic University ²Pennsylvania State University ³Tianjin University. Correspondence to: Lionel Z. WANG <zhe-leo.wang@connect.polyu.hk>.

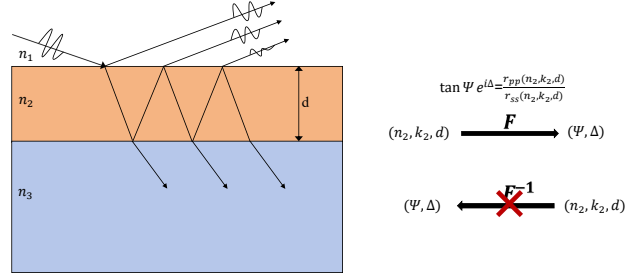


Figure 1. Schematic of light refraction in thin films and substrates. Light is incident onto a thin film with unknown optical constants and thickness (n_2, k_2, d) on a substrate with known optical constants (n_3, k_3) . Ellipsometry measures the parameters Ψ and Δ , with the forward mapping from (n_2, k_2, d) to (Ψ, Δ) . However, inverse mapping does not have an exact analytical formula and relies on data-fitting techniques.

ability to non-destructively measure the thickness and optical constants of thin films without the need for special sample preparation or damage to the sample, the simplicity of the method compared to other precision methods such as weighing and quantitative chemical analyses, and the ability of ellipsometry to measure very thin films (1 nm) with a high degree of accuracy, 1-2 orders of magnitude better than that of interferometric methods (Tompkins & Irene, 2005).

Ellipsometry-based measurements have limitations as they are indirect methods. We cannot directly calculate the optical constants and thickness of a thin film from the measured values of Δ and Ψ . Instead, it requires a complex process of data analysis and fitting (Collins et al., 2000). This involves iteratively adjusting the input values for the film’s optical constants and thickness to find the ellipsometric parameters that best match the experimental results. This process is highly time-consuming and labor-intensive, demanding considerable expertise from the operator.

The inverse ellipsometry problem is usually difficult to obtain an analytical solution, and the method of determining the optical constants and thicknesses of thin films by the fitting technique described above relies on the intervention of a human expert to provide an initial guess of the properties of the sample, which makes the ellipsometric polarisation anal-

ysis lengthy and time-consuming (Zhu et al., 2024). This is the main problem that we address, i.e., the use of neural networks to reconstruct the inverse ellipsometry problem, in addition to the fact that ellipsometry measurements are susceptible to interference from environmental factors such as temperature and humidity, which may lead to uncertainty in the results (Oates et al., 2011). Therefore, the development of a fast, economical and easy-to-operate method for the characterisation of optical properties of thin film materials is of great scientific significance and application value. In this context, the application of machine learning techniques to solve the inverse ellipsometry problem gradually comes into the spotlight.

In recent years, artificial intelligence, especially deep learning technology, is widely applied in the field of material and physics science (Butler et al., 2018; Wei et al., 2019), opening up new avenues for material property prediction and material design. We construct a large-scale benchmark dataset of thin film optical properties, encompassing 98 thin film materials and 4 substrate materials, with a total of over 8 million data points. This dataset is intended for other researchers to test their machine learning methods. The detailed construction process and description of the dataset are presented in Section 3. We test traditional machine learning methods on this dataset, including multilayer perceptrons, decision trees, random forests, and support vector machines. Additionally, we propose a deep learning-based framework, which achieves SOTA performance on this dataset.

When designing the network architecture, we are inspired by residual connections and the self-attention mechanism, incorporating both techniques into our framework to design a deep neural network. Additionally, during our experiments, we discover that our dataset exhibits one-to-many mapping relationships, meaning that in the training data, there might be various different thin films with the same thickness. This makes it challenging to achieve high thickness prediction accuracy on the validation and test sets if the network is optimized simply using a simple mean squared error loss function. This observation leads us to design a novel reconstruction loss function to guide the network’s parameter updates. This function is based on the forward ellipsometry formula (Kim et al., 2016), details in Section 4.3. In this way, we implicitly utilize the forward ellipsometry formula on top of the normal ground truth fitting, aiming to enable the neural network to learn the inverse mapping from ellipsometric parameters to optical constants and thin film thickness. During the design of the loss function, we employ numerical methods to replace complex number operations, ensuring that gradients can be computed smoothly. Details of the reconstruction loss can be found in Section 4.3.

Contributions

- Constructed a large-scale benchmark dataset of ellipsometry parameters and thin film optical properties.
- Proposed an effective deep learning framework to solve the inverse ellipsometry problem.
- Designed a novel reconstruction loss function to address the one-to-many mapping issue, improving prediction performance.

2. Related Work

Ellipsometry is a crucial technique for measuring the optical properties and thickness of thin films, widely used in semiconductor manufacturing and optoelectronic device fabrication. However, it only provides an indirect relationship between measured optical parameters and the actual properties of thin films, presenting a classic example of an inverse problem (Bell, 1978). These inverse problems are typically ill-posed, with challenges in ensuring the existence, uniqueness, and stability of solutions (Akbalk et al., 2009).

2.1. Mathematical-Inversion Method

Ellipsometry has inherent limitations as an indirect method for measuring thin film optical properties. The measured Δ and Ψ cannot be directly converted to optical constants and usually require a fitting process (Collins et al., 2000). Only for very thick, isotropic, and homogeneous films can Δ and Ψ be directly converted. In other cases, a multi-layer physics model is needed, considering the optical constants and thicknesses of all layers in the correct order. Using a multiple least-square optimization, the unknown optical constants (n_2, k_2) and thickness d are varied and substituted into the Fresnel equation to find Δ and Ψ (Whiteside et al., 2016). The final Δ and Ψ values that best match the experimental data yield the optimized optical constants and thicknesses. This process often requires multiple attempts by experts, making it time-consuming and labor-intensive, thus limiting the efficiency of ellipsometric measurements.

2.2. Machine-Learning Method

Recently, the rapid advancement of machine learning, particularly deep learning, has provided new methodologies for solving complex problems by learning from vast datasets, achieving notable success in areas such as computer vision and natural language processing (LeCun et al., 2015; He et al., 2016). Inspired by these developments, some researchers have integrated deep learning into the analysis of ellipsometric data. For instance, Urban et al. utilized artificial neural networks as preprocessors in the ellipsometric inversion process, providing improved initial values for subsequent regression fitting (Urban III & Tabet, 1994). While this method enhances computational speed, it still

Table 1. Film and substrate materials in the dataset

TYPE	CATEGORY	MATERIALS	
FILM	METAL	Ag, Al, Au, Be, Cd, Co, Cr, Cs, Cu, Fe, Hg, In, Ir, K, Li, Mg, Mn, Mo, Na, Nb, Ni, Os, Pd, Pt, Re, Rh, Sb, Si, Sn, Ta, Ti, V, W, Zr, Ru,	
	ALLOY	AlTi, AlTiC, In ₅₃ GaAs, NiFe, NiP, TiW	
	COMPOUND	Al ₂ O ₃ , AlAs, AlGaAs, AlN, AlSb, BaTiO ₃ , CaF ₂ , CdS, CdSe, CdTe, Cr ₂ O ₃ , Cu ₂ O, Fe ₂ O ₃ , GaAs, GaN, GaP, GaSb, CuO, Ge, HgSe, HgTe, In ₂ O ₃ , InAs, InGaAs, InN, InP, InSb, ITO, MgF ₂ , MgO, Mn ₂ O ₃ , Nb ₂ O ₅ , PbS, PbSe, PbTe, Si ₃ N ₄ , SiC, SiO, SiO ₂ , Ta ₂ O ₅ , Ta ₃ N ₅ , TaN, Te, ZrO ₂ , TiC, TiN, TiO ₂ , TiSi, VN, ZnS, ZnSe, ZrN,	
		POLYMER	PDMS, PMMA
		OTHERS	Glass, Diamond
		SUBSTRATE	COMPOUND

depends on conventional fitting optimizations and does not fundamentally eliminate the need for manual intervention.

Jiang et al. (2024) developed a deep-neural-network-assisted ellipsometry method for characterizing nano-gratings. They generated a dataset comprising 660,000 sets of randomly generated grating parameters and their corresponding ellipsometric data via numerical simulations. However, the specific types of materials used were not detailed, and the dataset was not publicly available. Arunachalam et al. (2022) proposed a machine learning-enhanced efficient spectroscopic ellipsometry modeling approach. While the exact size of their dataset was not specified, it included experimental and numerically simulated data of TiO₂ films. The dataset, however, was not publicly disclosed. Wang et al. (2022) introduced EllipsoNet, a deep-learning model for optical ellipsometry. Their dataset consisted of 450,000 multilayer stack structures, generating 90,000 input-output pairs using over 400 materials extracted from the C2DB database. Similarly, Wang et al. (2023) developed ReflectoNet, which also utilized 450,000 multilayer stack structures, generating 90,000 input-output pairs. This dataset included over 400 materials from the C2DB database. Liu et al. (2021) proposed a machine-learning approach for ellipsometry that relied on a dataset of 6240 pairs of values, derived from 200 materials listed in the Palik and Sopra databases. Although this dataset was well-documented, it was not openly shared.

To advance research in machine learning methods for ellipsometry, we have constructed a large-scale benchmark dataset of ellipsometric measurements, containing over 8 million entries across 400 different thin film materials, including metals, alloys, and compounds. This dataset serves as a significant contribution and a benchmark for future research, providing a comprehensive resource for training and evaluating machine learning models in the context of

ellipsometric analysis. metal 35, alloy 6, com 52, poly 2, others 2, compound 4 In this work, we propose a novel deep-learning approach for analyzing ellipsometric measurement data. We develop a framework capable of simultaneously predicting the optical constants and thickness of thin films, incorporating a novel reconstruction loss function to tackle the issue of multiple solutions in thickness prediction (Li et al., 2021).

3. EllipBench

In this section, we present a comprehensive overview of our dataset, detailing its sources, construction process, statistical information, and comparisons to existing datasets. This thorough description aims to provide clarity on the dataset’s robustness and its potential applications in the field of ellipsometric analysis.

3.1. Data Source

Our dataset comprises the optical constants, thin film thicknesses, and corresponding ellipsometric parameters of 98 thin film materials measured on four different substrate materials (a-Si, ITO, Si, SrTiO₃), detailed materials in Table 1. These thin films include metals, alloys, compounds, and organic polymers. The construction of our dataset proceeds as follows: initial data on the optical constants and thicknesses of the aforementioned thin films (measured by ellipsometry) are input into the forward model shown in Figure 1 to compute the corresponding ellipsometric parameters, thus forming the dataset. The optical constants and thicknesses of the thin films in the dataset were obtained from numerous past experiments conducted using ellipsometry.

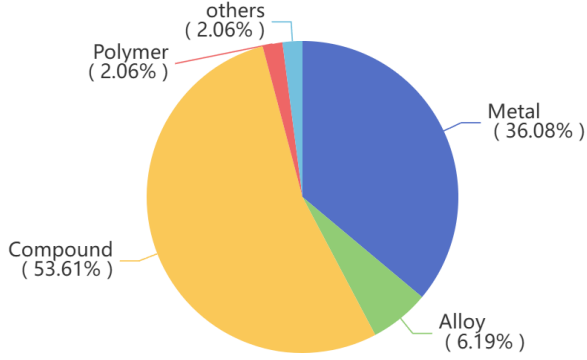


Figure 2. Data Distribution of EllipBench

3.2. Data Statistics

To ensure data diversity, our dataset also captures the variation in optical constants of the same material under different wavelengths, ranging from 380.28 nm to 999.87 nm. Additionally, to expand the dataset, we compute the ellipsometric parameters for varying film thicknesses, ranging from 1 nm to 96 nm, across 20 distinct thickness levels. Consequently, our dataset encompasses 8,296,200 entries, covering different material types, substrate materials, and optical parameters under various wavelengths, such as film thickness, optical constants, ellipsometric parameters, and the optical properties of the underlying substrates.

Furthermore, in our dataset partitioning, we design divisions among the 98 thin-film materials and the four substrate materials, as shown in Table 1, resulting in 392 material combinations. Each combination is divided in an 8:1:1 ratio into training, validation, and test sets. This division strategy ensures that our model can broadly learn the data mapping relationships across each material combination, thereby improving its adaptability and generalization performance when exposed to other materials. The distribution of dataset is presented in Figure 2.

3.3. Comparison with Existing Datasets

Jiang et al. (2024) create a dataset of 660,000 sets of grating parameters and corresponding ellipsometric data through numerical simulations. The specific materials used are not specified, and the dataset is not publicly available.

Arunachalam et al. (2022) include experimental and simulated data of TiO_2 films in their dataset. The dataset’s size is unspecified and is not publicly disclosed.

Wang et al. (2022) develop a dataset of 450,000 multilayer stack structures, resulting in 90,000 input-output pairs using over 400 materials from the C2DB database. This dataset is not publicly accessible.

Wang et al. (2023) also use 450,000 multilayer stack struc-

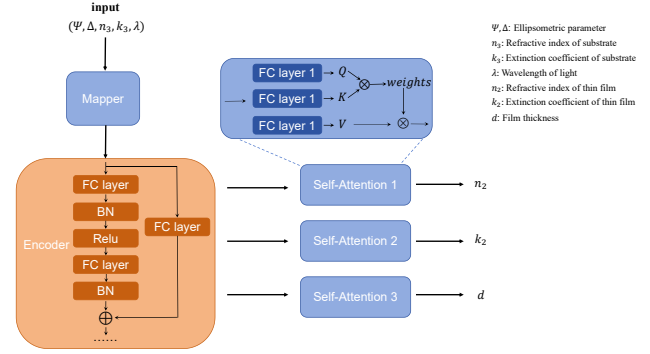


Figure 3. **Framework overview.** The proposed framework is built upon a deep neural network, with the encoder Θ_e consisting of 150 layers. The mapper Θ_m processes the input data, mapping it to a high-dimensional space to generate a feature map. The self-attention block then extracts important features from this feature map, F_e^a . Following the self-attention mechanism, the output values are obtained from the feature map by three separate projectors, each comprising a single fully connected layer. Both the reconstruction loss and the fitting loss collaboratively guide the mapper, the encoder, the self-attention block, and the projectors in updating their parameters.

tures, generating 90,000 input-output pairs from over 400 materials in the C2DB database. This dataset is not publicly available.

Liu et al. (2021) compile a dataset of 6240 pairs of (Ψ, Δ, R, T) and (n, k, d) values from 200 materials in the Palik and Sopra databases. This dataset is well-documented but not openly shared.

In summary, although there is extensive research on machine learning-based ellipsometry methods, most studies rely on small-scale datasets. Consequently, the trained models are often incomplete and may only learn the mapping relationships for a limited range of materials. This limitation affects the models’ generalization capabilities to other materials. Therefore, we propose a large-scale benchmark dataset that encompasses a broader range of materials and a significantly larger dataset size. This allows models to learn more comprehensive information, providing a solid foundation for future researchers.

4. Method

Unlike most existing work that relies on machine learning methods to solve the inverse ellipsometry problem, we have designed a framework based on deep neural network. In our design process, we draw inspiration from several classical methods. To address the issue of gradient vanishing in deep neural networks, we incorporated residual connections (He et al., 2016). For feature extraction, we utilized the self-attention mechanism (Vaswani et al., 2017). Additionally, the design of our reconstruction loss was inspired by the

classical encoder-decoder structures (Sutskever et al., 2014). The network structure is shown in Figure 3, and the detailed information of our DNN frame work will be introduced in Section 4.2.

4.1. Problem Statement

As shown in Figure 1, inverting the film thickness d and optical constants n_2 and k_2 from ellipsometry parameters Δ and Ψ is an ill-posed problem. Traditional mathematical fitting requires significant manual intervention and trial and error, making it inefficient and time-consuming (Fujiwara, 2007). This complexity contributes to the high learning curve and time cost of accurate, non-destructive ellipsometry. Our goal is to fit F^{-1} using deep learning methods.

To address this, we design a deep learning framework to map ellipsometry parameters to film thickness and optical constants (Li et al., 2021). We train our neural network by fitting its predictions to ground truth values of Δ , Ψ , n_2 , k_2 , and d using mean-square error. We also incorporate information from the forward computation formula F into the reconstruction loss, aiming for the network to learn the input-output mapping based on this formula.

The law of refraction. n_2 and k_2 represent the refractive index and extinction coefficient of the thin film material, respectively, while d represents the film thickness. n_3 and k_3 represent the refractive index and extinction coefficient of the substrate material. θ_i ($i=1,2,3$) represent the angles of refraction of light entering different materials. Here, N_1 , N_2 , and N_3 represent the complex refractive indices of air, the thin film, and the substrate, respectively. Both N_1 and θ_1 are known quantities.

$$\begin{aligned} N_2 &= n_2 + ik_2, \\ N_3 &= n_3 + ik_3, \\ N_1 \sin \theta_1 &= N_2 \sin \theta_2 = N_3 \sin \theta_3 \end{aligned} \quad (1)$$

Fresnel equation. r_p and r_s represent the reflectance of p-polarized and s-polarized light for a single-layer material, respectively. N and θ denote the negative refractive index and the angle of refraction for different materials. The subscripts up and down indicate their positions above or below in the layer model.

$$\begin{aligned} r_p &= \frac{N_{\text{down}} \cos \theta_{\text{up}} - N_{\text{up}} \cos \theta_{\text{down}}}{N_{\text{down}} \cos \theta_{\text{up}} + N_{\text{up}} \cos \theta_{\text{down}}}, \\ r_s &= \frac{N_{\text{up}} \cos \theta_{\text{up}} - N_{\text{down}} \cos \theta_{\text{down}}}{N_{\text{up}} \cos \theta_{\text{up}} + N_{\text{down}} \cos \theta_{\text{down}}} \end{aligned} \quad (2)$$

r_{pp} and r_{ss} indicate the refractive indices of perpendicularly and parallel polarized light in a double-layer structure, respectively. The subscripts r_p and r_s on the right-hand side of the equation represent the reflectance of perpendicularly

polarized and parallel polarized light from a single layer of material in different layer structures.

$$\begin{aligned} r_{pp} &= f(n_2, k_2, n_3, k_3, d, \Delta, \Psi, \lambda) \\ &= \frac{r_p(1, 2) + r_p(2, 3) \exp(-i2\beta)}{1 + r_p(1, 2)r_p(2, 3) \exp(-i2\beta)}, \\ r_{ss} &= g(n_2, k_2, n_3, k_3, d, \Delta, \Psi, \lambda) \\ &= \frac{r_s(1, 2) + r_s(2, 3) \exp(-i2\beta)}{1 + r_s(1, 2)r_s(2, 3) \exp(-i2\beta)} \end{aligned} \quad (3)$$

β indicates the phase difference between adjacent reflected beams. λ represents the wavelength of light.

$$\beta = 2\pi \left(\frac{d}{\lambda} \right) N_2 \cos \theta_2 \quad (4)$$

Establishes the mapping relationship between the refractive index, extinction coefficient, and thickness of thin films and the ellipsometric parameters.

$$\tan \Psi \exp(i\Delta) = \frac{r_{pp}}{r_{ss}}, \quad (5)$$

4.2. Network Architecture

In this section, we will provide a detailed explanation of the functions of each component in the network structure shown in Figure 3, including the network mapper, the encoder, three self-attention blocks, and three projectors.

Mapper The purpose of designing the mapper Θ_m is to map the input five dimensional features $(\Delta, \Psi, n_3, k_3, \lambda)$ to a higher dimensional space after non-linear combination and transformation.

$$F_m = \Theta_m(\Delta, \Psi, n_3, k_3, \lambda) \quad (6)$$

Given the dataset size of approximately eight million entries, the original feature space is relatively limited. Therefore, to enhance the feature representation, the mapper employs a structure of convolutional, pooling, and fully connected layers. The mapper enables the transformation of input features into a higher dimensional space, where non-linear mapping facilitates the extraction of more informative features for downstream processing.

Encoder The encoder Θ_e , the backbone of the network, is a deep neural network that includes multiple fully connected layers, convolutional layers, and pooling layers. It incorporates the concept of residual connection to mitigate issues related to network degradation due to excessive depth, including gradient vanishing and exploding problems (He et al., 2016). This design not only accelerates network convergence but also enables the encoder to compress the high-dimensional inputs from the mapper into potent spatial representations.

$$F_e = \Theta_e(F_m) \quad (7)$$

By doing so, the network is forced into learning the most salient features.

Attention Block We design a separate projector Θ_p^i and self-attention block for each output value. Given that each output value has its own unique physical meaning, we create distinct self-attention blocks and projectors for each to effectively extract useful features from the encoder’s feature maps (Vaswani et al., 2017). This approach not only enhances the interpretability of the network but also significantly improves predictive performance.

In designing the self-attention block, we utilize the classical self-attention mechanism. Specifically, for the input feature map, three linear fully connected layers are employed to compute the query, key, and value. The attention score of the feature map is then computed according to Equation (8), normalized by the softmax function (Mnih et al., 2014), and the value is calculated as an inner product. This process results in a feature map with the appropriate attention weights.

$$F_e^a = \text{softmax}\left(\frac{Q \cdot K^\top}{\sqrt{d_k}}\right) \cdot V \quad (8)$$

Finally, the weighted feature maps are fed into each of the three projectors to obtain the output values.

$$\text{output}_i = \Theta_p^i(F_e^a) \quad (9)$$

4.3. Loss

In this section, we introduce the computational methodologies and functional roles of two pivotal loss functions employed within our proposed DNN framework: the fitting loss and the reconstruction loss.

Fitting Loss The fitting loss is a quintessential component in regression tasks, quantifying the discrepancy between the predicted outputs and the true labels. Specifically, the predicted values $(\widehat{n}_2, \widehat{k}_2, \widehat{d})$ correspond to the real labels (n_2, k_2, d) . The fitting loss function is defined as follows:

$$\text{FitLoss} = \frac{1}{3} \left((\widehat{n}_2 - n_2)^2 + (\widehat{k}_2 - k_2)^2 + (\widehat{d} - d)^2 \right) \quad (10)$$

The fitting loss, commonly used in regression tasks, measures the deviation between predicted and ground truth values (Panchal et al., 2011). Minimizing this loss via back-propagation helps the neural network align its outputs with true values. This encourages learning features necessary for mapping optical properties of the substrate and ellipsometry parameters to those of the thin film material. However, due to the dataset’s distribution, one-to-many mapping relationships exist between inputs and outputs (Wu et al., 2023). Thus, relying solely on fitting loss is insufficient for effective learning. Additionally, the prediction accuracy for

output value d is unsatisfactory, prompting the design of a reconstruction loss.

Reconstruction Loss To design the reconstruction loss, we adopt the tandem neural network structure proposed by Liu et al. (2017), which addresses the training difficulties of deep neural networks in inverse design by connecting a forward modeling network and an inverse design network in tandem. This structure overcomes the issue of non-unique mapping between the input and output of the neural network (Prince, 2023). Specifically, the forward modeling network captures the response variations corresponding to small differences between structures by learning the complex mapping relationships between structural parameters and electromagnetic responses. The inverse design network utilizes this information to select the structure that best matches the desired response. By connecting these networks in series and leveraging their interaction, the tandem structure provides additional constraints and guidance, enabling the inverse design network to accurately invert the structure that meets the requirements.

However, in the method proposed by Liu et al. (2017), pre-training of the forward network is necessary, and the parameters of the forward network are frozen during the training of the inverse network. Additionally, the performance of the inverse network highly depends on the performance of the forward network (Bolukbasi et al., 2017). Consequently, this scheme is time-consuming and limited in accuracy. To address these limitations, we have made improvements based on their method. In our problem, the mapping from the optical properties of the thin film material to the ellipsometric parameters is known and accurate. The process of forward computation is represented inside the reconstruction loss function (Xu et al., 2023). Thus, we can eliminate the process of training the forward network, resulting in an end-to-end framework with higher accuracy. The reconstruction loss function is defined as follows.

Inputs and outputs of model:

$$\begin{aligned} \text{inputs} &= (n_3, k_3, \lambda, \Psi, \Delta), \\ \text{outputs} &= (\widehat{n}_2, \widehat{k}_2, \widehat{d}) \end{aligned} \quad (11)$$

Calculation of reconstruction loss. Since it is difficult to directly compute the mean square error between complex numbers, we choose to compute the mean square error for the real and imaginary parts separately respectively. $\Re()$ and $\Im()$ represent the real and imaginary parts of a complex number, respectively.

$$\begin{aligned} \widehat{r}_{pp} &= f(\widehat{n}_2, \widehat{k}_2, n_3, k_3, \widehat{d}, \Delta, \Psi, \lambda), \\ \widehat{r}_{ss} &= g(\widehat{n}_2, \widehat{k}_2, n_3, k_3, \widehat{d}, \Delta, \Psi, \lambda), \end{aligned} \quad (12)$$

$$Loss = \frac{1}{2} \left[\left(\Re \left(\frac{\widehat{r}_{pp}}{\widehat{r}_{ss}} \right) - \Re (\tan \Psi \exp(i\Delta)) \right)^2 + \left(\Im \left(\frac{\widehat{r}_{pp}}{\widehat{r}_{ss}} \right) - \Im (\tan \Psi \exp(i\Delta)) \right)^2 \right] \quad (13)$$

5. Experiments

In this section, we first compare the performance of our proposed framework with traditional machine learning methods on the given dataset, demonstrating that our approach achieves SOTA results on this dataset. Next, we select a representative material from each category and use line charts to specifically illustrate the model’s prediction performance. Additionally, we test the model’s performance on untrained materials. Finally, we conduct ablation studies to demonstrate the importance and role of each component in our framework.

5.1. Implementation Details

Our training process is conducted in an environment with PyTorch 2.0.0, CUDA 11.8, and Python 3.10. The optimizer used for our model is Adam, with a learning rate of 1×10^{-5} and a weight decay of 1×10^{-4} . We set the batch size to 2048. The dataset is split into training, validation, and test sets with a ratio of 8:1:1. During data splitting, we ensure that each type of material is evenly and randomly sampled into the training set, allowing the model to learn from all material types adequately.

Our model features a 150-layer encoder, which includes fully connected layers, batch normalization, and residual connections. The activation function used is ReLU. For the self-attention mechanism module, we employ three fully connected layers (2048x2048) to compute the query, key, and value values. For testing traditional machine learning methods, we utilize various algorithms from the scikit-learn library, with all model parameters set to their default values.

5.2. Evaluation Metrics

In our experiments, we selected four evaluation metrics to assess the performance of the model. These metrics are Mean Absolute Error (MAE), the coefficient of determination (R^2), and accuracy. Accuracy is determined by considering a prediction correct if the difference between the predicted value and the true value is less than 0.05.

5.3. Comparison with ML Methods

In this section, we compare the decision tree regression model, random forest regression model, ElasticNet regression model, and multilayer perceptron regression model as baseline models with our proposed framework. These machine learning methods have been traditionally employed

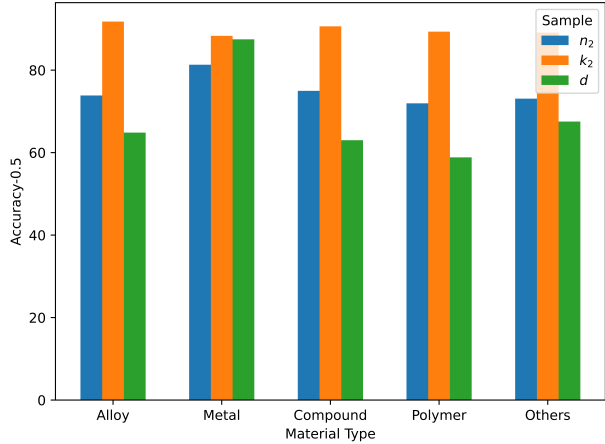


Figure 4. Generalization on Unknown Materials

to solve inverse ellipsometry problems (Arunachalam et al., 2022). All machine learning models are set to use default parameters. The results of our experiments are presented in Table 1.

The deep neural network framework we proposed significantly outperforms traditional machine learning methods on the dataset. Particularly in predicting film thickness, our framework shows remarkable superiority, primarily due to the reconstruction loss function we designed.

5.4. Generalization on Unknown Materials

Since materials with different thicknesses will show very different results when measured with ellipsometry, we tested 96 thin film materials, we tested 96 types of thin film materials, each with three different thicknesses (Collins & Kim, 1990). Using this test dataset, we evaluated the generalization performance of our model. The test results indicate that the model performs well on untrained datasets at a 0.5 precision level, particularly in predicting metallic materials. However, the accuracy at 0.05 or 0.1 precision levels is not satisfactory, which is an area we aim to improve in the future. Results. The results are detailed in Figure 4.

5.5. Ablation Study

To understand the impact of different components in our proposed model, we conduct an ablation study. Specifically, we evaluate the performance of models with varying encoder depths (50 layers, 100 layers, and our proposed 150 layers) (Pathak et al., 2016), the use of self-attention modules, and the inclusion of reconstruction loss. The results are summarized in Table 2.

From the table, several observations can be made:

Table 2. Ablation study results comparing different components

MODEL	ACCURACY n_2	ACCURACY k_2	ACCURACY d	MAE	R ²
OURS (ENCODER-50-LAYERS)	87.73%	96.72%	66.16%	0.305	0.9378
OURS (ENCODER-100-LAYERS)	75.43%	95.02%	63.99%	0.329	0.9384
OURS (WITHOUT SELF-ATTENTION)	86.15%	97.40%	76.66%	0.261	0.9396
OURS (WITHOUT RECONSTRUCTION LOSS)	96.51%	97.36%	62.50%	0.332	0.9588
OURS (OURS)	98.01%	98.66%	82.56%	0.192	0.9474

Table 3. Comparison results of our framework with baseline models

MODEL	ACCURACY n_2	ACCURACY k_2	ACCURACY d	MAE	R ²
DECISIONTREE	75.43%	87.17%	27.56%	0.774	0.8675
SVM	89.64%	90.88%	52.89%	0.599	0.7979
RANDOMFOREST	76.11%	87.31%	37.40%	0.663	0.7755
ELASTICNET	2.55%	90.84%	9.99%	1.772	0.0001
OURS	98.01%	98.66%	82.56%	0.192	0.9674

- **Encoder Depth:** Increasing the depth of the encoder generally improves performance. Our proposed model with 150 layers achieves the highest accuracies across all metrics, with an accuracy n_2 of 98.01%, accuracy k_2 of 98.66%, and accuracy d of 82.56%. Additionally, it achieves the lowest MAE (0.192).
- **Self-Attention Block:** The inclusion of the self-attention block significantly enhances the model’s performance. The model without self-attention shows a decrease in performance, especially in accuracy d (76.66% compared to 82.56% for our model).
- **Reconstruction Loss:** Incorporating reconstruction loss also positively impacts the performance. The model without reconstruction loss, shows a drop in Accuracy d (62.50%) and higher MAE (0.332) compared to our proposed model.

Overall, these results validate the effectiveness of our proposed 150-layer encoder with self-attention block and reconstruction loss, demonstrating superior performance in terms of accuracy and error metrics.

6. Conclusion

In this paper, we address the challenges of traditional ellipsometry by introducing a large-scale benchmark dataset, which includes 98 types of thin film materials and 4 types of substrate materials, totaling over 8 million data points. This dataset is a significant contribution to the field, providing a valuable resource for the development and testing of machine learning methods.

The proposed deep learning framework incorporates residual connections and self-attention mechanisms, achieving

state-of-the-art performance on our dataset. A key innovation is the reconstruction loss function, which effectively handles the one-to-many mapping problem in thin film thickness prediction, enhancing the network’s accuracy. Our results demonstrate that the proposed framework not only surpasses traditional machine learning methods but also simplifies the ellipsometry process, reducing the need for extensive human expertise and time. This advancement makes ellipsometry more accessible and efficient for various industrial applications.

In summary, our large-scale benchmark dataset and deep learning framework advance the application of machine learning to solving the inverse ellipsometry problem, facilitating more accurate and efficient thin film characterization.

References

- Akbalık, A., Soulan, S., Tortai, J.-H., Fuard, D., Kone, I., Hazart, J., and Schiavone, P. An inverse ellipsometric problem for thin film characterization: comparison of different optimization methods. In *Metrology, Inspection, and Process Control for Microlithography XXIII*, volume 7272, pp. 1122–1128. SPIE, 2009.
- Arunachalam, A., Berriel, S. N., Banerjee, P., and Basu, K. Machine learning-enhanced efficient spectroscopic ellipsometry modeling. *arXiv preprint arXiv:2201.04933*, 2022.
- Bell, J. B. Solutions of ill-posed problems., 1978.
- Bolukbasi, T., Wang, J., Dekel, O., and Saligrama, V. Adaptive neural networks for efficient inference. In *International Conference on Machine Learning*, pp. 527–536. PMLR, 2017.

- Butler, K. T., Davies, D. W., Cartwright, H., Isayev, O., and Walsh, A. Machine learning for molecular and materials science. *Nature*, 559(7715):547–555, 2018.
- Collins, R., Koh, J., Fujiwara, H., Rovira, P., Ferlauto, A., Zapfen, J., Wronski, C., and Messier, R. Recent progress in thin film growth analysis by multichannel spectroscopic ellipsometry. *Applied surface science*, 154: 217–228, 2000.
- Collins, R. W. and Kim, Y.-T. Ellipsometry for thin-film and surface analysis. *Analytical Chemistry*, 62(17):887A–900A, 1990.
- Fujiwara, H. *Spectroscopic ellipsometry: principles and applications*. John Wiley & Sons, 2007.
- He, K., Zhang, X., Ren, S., and Sun, J. Deep residual learning for image recognition. In *Proceedings of the IEEE conference on computer vision and pattern recognition*, pp. 770–778, 2016.
- Jiang, Z., Gan, Z., Liang, C., and Li, W.-D. Generic characterization method for nano-gratings using deep-neural-network-assisted ellipsometry. *Nanophotonics*, (0), 2024.
- Kim, C., Piloni, G., and Ramprasad, R. Machine learning assisted predictions of intrinsic dielectric breakdown strength of abx₃ perovskites. *The Journal of Physical Chemistry C*, 120(27):14575–14580, 2016.
- LeCun, Y., Bengio, Y., and Hinton, G. Deep learning. *nature*, 521(7553):436–444, 2015.
- Li, Y., Wu, Y., Yu, H., Takeuchi, I., and Jaramillo, R. Deep learning for rapid analysis of spectroscopic ellipsometry data. *Advanced Photonics Research*, 2(12):2100147, 2021.
- Liu, D., Tan, Y., Khoram, E., and Yu, Z. Training deep neural networks for the inverse design of nanophotonic structures. *arXiv e-prints*, art. arXiv:1710.04724, October 2017. doi: 10.48550/arXiv.1710.04724.
- Liu, J., Zhang, D., Yu, D., Ren, M., and Xu, J. Machine learning powered ellipsometry. *Light: Science & Applications*, 10(1):55, 2021.
- Mnih, V., Heess, N., Graves, A., et al. Recurrent models of visual attention. *Advances in neural information processing systems*, 27, 2014.
- Oates, T., Wormeester, H., and Arwin, H. Characterization of plasmonic effects in thin films and metamaterials using spectroscopic ellipsometry. *Progress in Surface Science*, 86(11-12):328–376, 2011.
- Panchal, G., Ganatra, A., Shah, P., and Panchal, D. Determination of over-learning and over-fitting problem in back propagation neural network. *International Journal on Soft Computing*, 2(2):40–51, 2011.
- Pathak, D., Krahenbuhl, P., Donahue, J., Darrell, T., and Efros, A. A. Context encoders: Feature learning by inpainting. In *Proceedings of the IEEE conference on computer vision and pattern recognition*, pp. 2536–2544, 2016.
- Prince, S. J. *Understanding Deep Learning*. MIT press, 2023.
- Sutskever, I., Vinyals, O., and Le, Q. V. Sequence to sequence learning with neural networks. *Advances in neural information processing systems*, 27, 2014.
- Tompkins, H. and Irene, E. A. *Handbook of ellipsometry*. William Andrew, 2005.
- Urban III, F. K. and Tabet, M. F. Real time, in-situ ellipsometry solutions using artificial neural network pre-processing. *Thin Solid Films*, 245(1-2):167–173, 1994.
- Vaswani, A., Shazeer, N., Parmar, N., Uszkoreit, J., Jones, L., Gomez, A. N., Kaiser, L., and Polosukhin, I. Attention is all you need. *Advances in neural information processing systems*, 30, 2017.
- Wang, Z., Lin, Y. C., Zhang, K., Wu, W., and Huang, S. Ellipsonet: Deep-learning-enabled optical ellipsometry for complex thin films. *arXiv preprint arXiv:2210.05630*, 2022.
- Wang, Z., Lin, Y. C., Zhang, K., Wu, W., and Huang, S. Measuring complex refractive index through deep-learning-enabled optical reflectometry. *2D Materials*, 10(2):025025, 2023.
- Wei, J., Chu, X., Sun, X.-Y., Xu, K., Deng, H.-X., Chen, J., Wei, Z., and Lei, M. Machine learning in materials science. *InfoMat*, 1(3):338–358, 2019.
- Whiteside, P. J., Chininis, J. A., and Hunt, H. K. Techniques and challenges for characterizing metal thin films with applications in photonics. *Coatings*, 6(3):35, 2016.
- Wu, H., Hu, T., Luo, H., Wang, J., and Long, M. Solving high-dimensional pdes with latent spectral models. *arXiv preprint arXiv:2301.12664*, 2023.
- Xu, Y., Kohtz, S., Boakye, J., Gardoni, P., and Wang, P. Physics-informed machine learning for reliability and systems safety applications: State of the art and challenges. *Reliability Engineering & System Safety*, 230: 108900, 2023.

Zhu, P., Zhang, D., Niu, X., Liu, J., Ren, M., and Xu, J. A lightweight neural network for spectroscopic ellipsometry analysis. *Advanced Optical Materials*, pp. 2301381, 2024.